A NEW LAMINATED OVERBURDEN MODEL FOR COAL MINE DESIGN

By Keith A. Heasley[1]

ABSTRACT

In the past, numerous boundary-element models of stratified rock masses have been proposed using a homogeneous isotropic elastic overburden. In this paper, it is postulated that a laminated overburden model might be more accurate for describing the displacements and stresses in these stratified deposits. In order to investigate the utility of using a laminated overburden in a boundary-element model, the fundamental mathematical basis of the laminated model is presented and graphically compared with the fundamental behavior of homogeneous isotropic elastic overburden and with field data. Specifically, the stresses and displacements surrounding an idealized longwall panel as determined from the laminated overburden model are presented and compared with results from the homogeneous isotropic overburden and with measured abutment stress data. Additionally, the remote displacements and surface subsidence as calculated by the laminated overburden model are compared with homogeneous isotropic calculations and with measured subsidence data. Finally, the new laminated boundary-element program, LAMODEL, is used to model the underground stresses and displacements, the topographic stresses, and the interseam interactions at a field site. The results of this investigation show that the laminated overburden is more supple, apt to propagate displacements and stress further, and better able to fit observed data than the classic homogeneous isotropic overburden. Ultimately, it is suggested that the laminated model has the potential to increase the accuracy of displacement and stress calculations for a variety of mining situations.

[1]Mining engineer, Pittsburgh Research Center, National Institute for Occupational Safety and Health, Pittsburgh, PA.

INTRODUCTION

If one wishes to perform a mechanical analysis of the geologic structure of a mining operation, there are several broad mathematical techniques available. For instance, one may choose finite-element, boundary-element, discrete-element, finite-difference techniques, and/or hybrid combinations of these techniques. In general, these mathematical techniques have strengths and weaknesses when applied to a specific geologic environment, mining geometry, and material behavior. Naturally, in each practical application the mathematical technique best suited to the prevailing conditions should be applied.

To analyze the displacements and stresses associated with the extraction of tabular deposits, such as coal, potash, and other thin vein-type deposits, the displacement-discontinuity version of the boundary-element technique is frequently the method of choice. In the displacement-discontinuity approach, the mining horizon is treated mathematically as a discontinuity in the displacement of the surrounding media. Thus, only the planar area of the seam is discretized in order to obtain the solution. Often this limited analysis is sufficient, because in many applications only the distributions of stress and convergence on the seam horizon are of interest. In addition, by limiting the detailed analysis to only the seam, the displacement-discontinuity method provides considerable computational savings compared with other techniques that discretize the entire body (such as finite-element, discrete-element, or finite-difference). It is a direct result of this computational efficiency that the displacement-discontinuity method is able to handle problems involving large areas of tabular excavations.

In the original mathematical formulations [Berry 1960; Salamon 1962] and computer implementations [Plewman et al. 1969; Crouch and Fairhurst 1973; Sinha 1979] of the displacement-discontinuity variation of the boundary-element method, the media surrounding the seam were assumed to be homogeneous, isotropic, or transversely isotropic elastic. This basic behavior of the surrounding media provided fairly good seam-level displacement and stress results for South African gold mines [Salamon 1964; Cook et al. 1966] and for U.S. coal mines [Kripakov et al. 1988; Zipf and Heasley 1990; Heasley and Zclanko 1992]. However, it was noted early in the application of the displacement-discontinuity method that the homogeneous isotropic overburden model does not fit measured subsidence data [Berry and Sales 1961]. As an alternative, it was proposed that a laminated model might be more suitable for describing the behavior of stratified coal-measure rocks [Salamon 1961, 1963]. Recently, a laminated overburden model was found to give good results for predicting surface subsidence [Salamon 1989a; Yang 1992]. Because the source of surface subsidence is convergence in the seam, it seems reasonable that a laminated overburden model might also be able to provide more accurate predictions of in-seam displacements and stresses.

If the utility of using a laminated overburden in a displacement-discontinuity model is to be determined, the fundamental mechanical behavior of the laminated model needs to be investigated and compared with both the classic homogeneous isotropic model and field data. In this paper, the stresses and displacements surrounding an idealized longwall panel as determined from the laminated overburden model, the homogeneous isotropic overburden model, and field data are presented and compared. In addition, the remote displacements and surface subsidence as calculated by the two overburden models are compared with measured subsidence data. Lastly, the laminated overburden model is applied to a site study.

FUNDAMENTAL BEHAVIOR

MATHEMATICAL FOUNDATION

The mathematical basis for the laminated model was originally proposed by Salamon in 1961-62 and more recently updated in 1991. Conceptually, the media in the laminated model consist of a horizontal stack of homogeneous isotropic layers where the interfaces between the layers are parallel and free of shear and cohesive stresses, and the vertical stresses and displacements are continuous across the layers. In the "homogeneous stratification" version of the model, all layers have the same elastic modulus (E), Poisson's ratio (v), and thickness (t). Thus, the homogeneous stratification formulation does not allow (or need) the specification of the properties for each individual layer, yet it provides the desired suppleness of the basic laminated model (compared with a homogeneous isotropic elastic model). In addition, the behavior of the rock mass in the laminated model is effectively characterized by two parameters, the elastic modulus and the lamination thickness, whereas the homogeneous isotropic model only has a single effective parameter, the rock mass modulus (the Poisson's ratio has a minor effect in both models).

The mathematical foundation of the laminated model is the theory of thin plates [Salamon 1991]. From this theory, the relationship between the vertical deflection (w) of the middle plane of a horizontal plate and the resultant transverse pressure (p) acting on the plate is defined by

$$D \nabla^4 w(x,y) = p(x,y), \quad (1)$$

where D is the flexural rigidity of a plate:

$$D = \frac{E t^3}{12 (1 - \nu^2)}, \quad (2)$$

and ∇^4 denotes the biharmonic operator in the xy plane, specifically:

$$\nabla^4 = \left(\frac{\partial^4}{\partial x^4} + 2 \frac{\partial^4}{\partial x^2 \partial y^2} + \frac{\partial^4}{\partial y^4} \right). \quad (3)$$

From equation 1, the convergence in the seam (S) can be related to the induced stress (σ_i) in the overburden laminae by the following second-order, partial differential equation [Salamon 1991]:

$$\frac{\partial^2 S}{\partial x^2} + \frac{\partial^2 S}{\partial y^2} = \frac{2}{E \lambda} \sigma_i, \quad (4)$$

where the laminae-related value, λ, is defined as

$$\lambda = \sqrt{\frac{t^2}{12 (1 - \nu^2)}}, \quad (5)$$

and σ_i is the vertical, or transverse, stress on the laminae at seam level induced by mining.

PANEL CONVERGENCE

The first step in investigating the fundamental behavior of the laminated model was to analyze the convergence across a two-dimensional slot. This slot can be viewed as an idealized longwall panel with no gob support and rigid ribs. From equation 4, the seam convergence across a two-dimensional slot for the laminated model (S_ℓ) as a function of the distance from the panel centerline (X) can be determined as

$$S_\ell (X) = \frac{\sqrt{12 (1 - \nu^2)}}{t} \frac{q}{E} (L^2 - X^2). \quad (6)$$

Here, L is the half-width of the slot; q is the primitive vertical stress at the mining horizon, which for an open panel is equal to the induced stress (σ_i). In solving equation 4, it was assumed that the convergence value at the rib side is zero and that the convergence distribution is symmetric about the panel centerline. Also, in this result and the result in equation 7, the stress-free ground surface was ignored.

Jaeger and Cook [1979] provide a comparable equation for the roof-to-floor convergence across a two-dimensional slot with homogeneous isotropic elastic overburden (S_h):

$$S_h (X) = 4 (1 - \nu^2) \frac{q}{E} (L^2 - X^2)^{1/2}. \quad (7)$$

The fundamental difference between these two equations is that the convergence in the laminated model is proportional to the square of the panel span, while the convergence in the homogeneous model is linearly proportional to the span.

In order to plot and compare the convergence computed from equations 6 and 7, some "typical" values were assumed for the geometric and rock mass parameters: a panel width of 200 m (656 ft)(L = 100), an overburden depth (H) of 160 m (525 ft)(q = 4 MPa (580 psi)), a seam height (M) of 2 m (6.6 ft), an elastic modulus of the rock mass (E) of 20 GPa (2.9 million psi), a Poisson's ratio (ν) of the rock mass of 0.25, and a lamination thickness (t) of 15 m (49 ft). Using these values for the parameters, the convergence across the slot for both the laminated and the homogeneous overburden is plotted in figure 1. As expected from the nature of the equations, the laminated overburden is considerably more flexible. In fact, with the given parameters, the laminated overburden exhibits six times the convergence of the homogeneous isotropic overburden.

ABUTMENT STRESS

The next step in investigating the fundamental behavior of the laminated model was to analyze the abutment stress at the edge of a two-dimensional slot. If the seam is assumed to be linear elastic with a modulus of E_s and Poisson's effect is ignored, then the induced stress in the seam for the laminated model is

$$\sigma_i = E_s \frac{S_\ell}{M}. \quad (8)$$

Then, from equation 4, the in-seam convergence in the laminated model is defined by

$$\frac{d^2 S_\ell}{dx^2} - \frac{2 E_s}{E \lambda M} S_\ell = 0, \quad (9)$$

which has a solution (for positive X values):

$$S_\ell (X) = qL \sqrt{\frac{2M}{E \lambda E_s}} e^{\sqrt{\frac{2E_s}{E \lambda M}} (X-L)}. \quad (10)$$

The associated induced vertical abutment stress (σ_ℓ) in the unmined seam bounding the panel is

$$\sigma_\ell (X) = qL \sqrt{\frac{2E_s}{E \lambda M}} e^{\sqrt{\frac{2E_s}{E \lambda M}} (X-L)}. \quad (11)$$

The total abutment stress at the edge of a two-dimensional slot in a homogeneous isotropic elastic model (σ_h) is given by [Salamon 1974]:

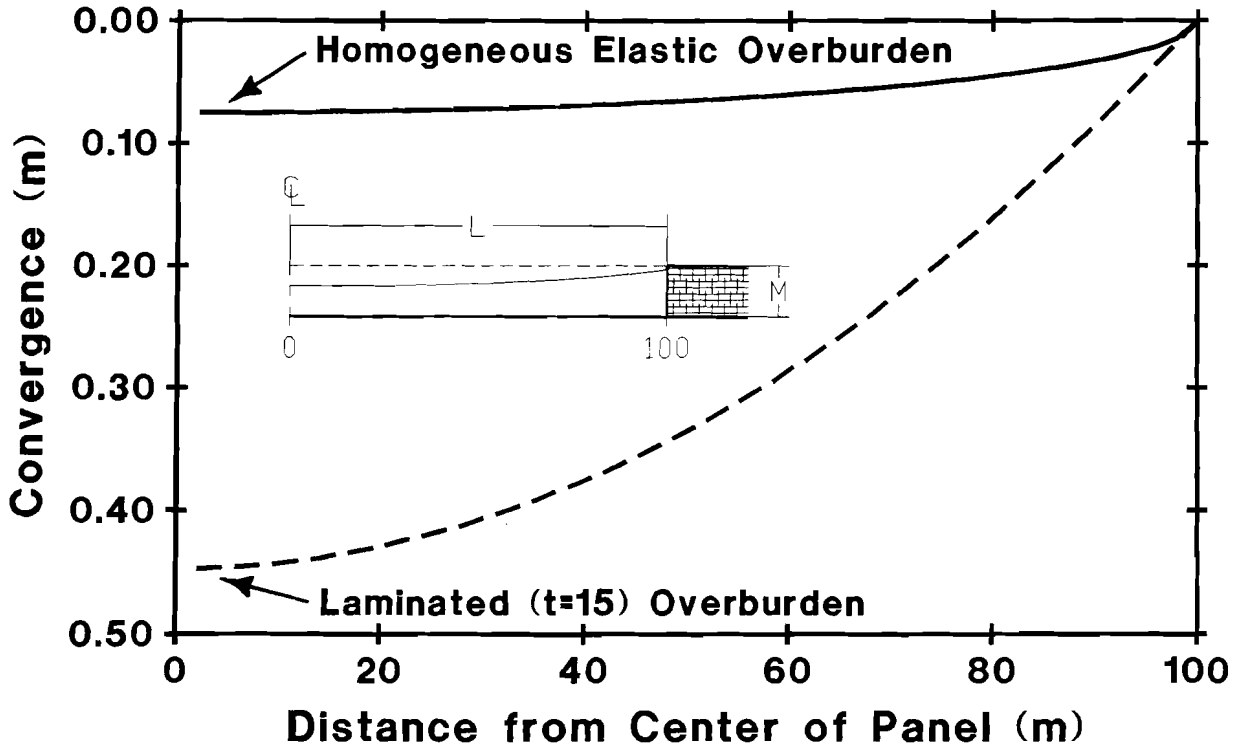

Figure 1.—Comparison of longwall convergence computed from the laminated and homogeneous isotropic models.

$$\sigma_h(X) = \frac{Xq}{\sqrt{X^2 - L^2}}. \qquad (12)$$

It is noteworthy that this equation is independent of material properties. During its derivation, it was assumed that the seam material was identical to the surrounding media. Thus, to be consistent, the elastic modulus of the seam (E_s) in equation 11 is assumed to be equal to the modulus of the overburden (E), 20 GPa (2.9 million psi).

In addition, numerous field measurements of abutment load have been tabulated by Mark [1990], where he found that the measured distribution of induced abutment stress (σ_f) follows the equation:

$$\sigma_f(X) = \frac{3L_s}{(D - L)^3}(D - X)^2, \qquad (13)$$

where L_s is the total side abutment load (which in our case without any gob load is equal to qL), and D is the maximum horizontal extent of the abutment stress from the panel edge, which was determined from field measurements [Mark 1990]:

$$D = L + \sqrt{0.3048}(9.3\sqrt{H}). \qquad (14)$$

The total abutment stress curves, as calculated from the laminated and homogeneous isotropic models and from the empirical formula (equations 11, 12, and 13), are plotted in figure 2. (It should be noted that equations 11 and 13 calculate induced stresses and equation 12 calculates the total stress. Therefore, in the following plots, the virgin overburden stress (q) has been added to the results from equations 11 and 13 to provide a valid comparison with the total abutment stress values from equation 12.) In figure 2, it can be seen that the homogeneous isotropic abutment stress has a relatively sharp, infinite peak at the edge and approaches zero asymptotically with increasing distance from the panel. In contrast, the abutment stress in the laminated overburden is finite at the panel edge and approaches virgin overburden stress (q) rapidly. Neither of these mathematical models (using the assumed parameters) comes very close to matching the empirical abutment stress.

However, if the abutment stress level in the laminated model and that obtained from the empirical formula are equated at the edge of the seam (X = L), then the lamination thickness (t) that ensures this equality can be determined:

$$t = 20.29\sqrt{1 - v^2}\,\frac{E_s H}{M E}. \qquad (15)$$

For a typical seam modulus (E_s) of 2 GPa (290,000 psi) in the laminated model, equation 15 provides a fitted lamination thickness of 157 m (515 ft). The plot of the abutment stress curve for the laminated overburden model with a fitted lamination thickness of 157 m (515 ft) is shown together with the empirically determined abutment stress in figure 3. The degree of agreement between the two curves is very good and serves to

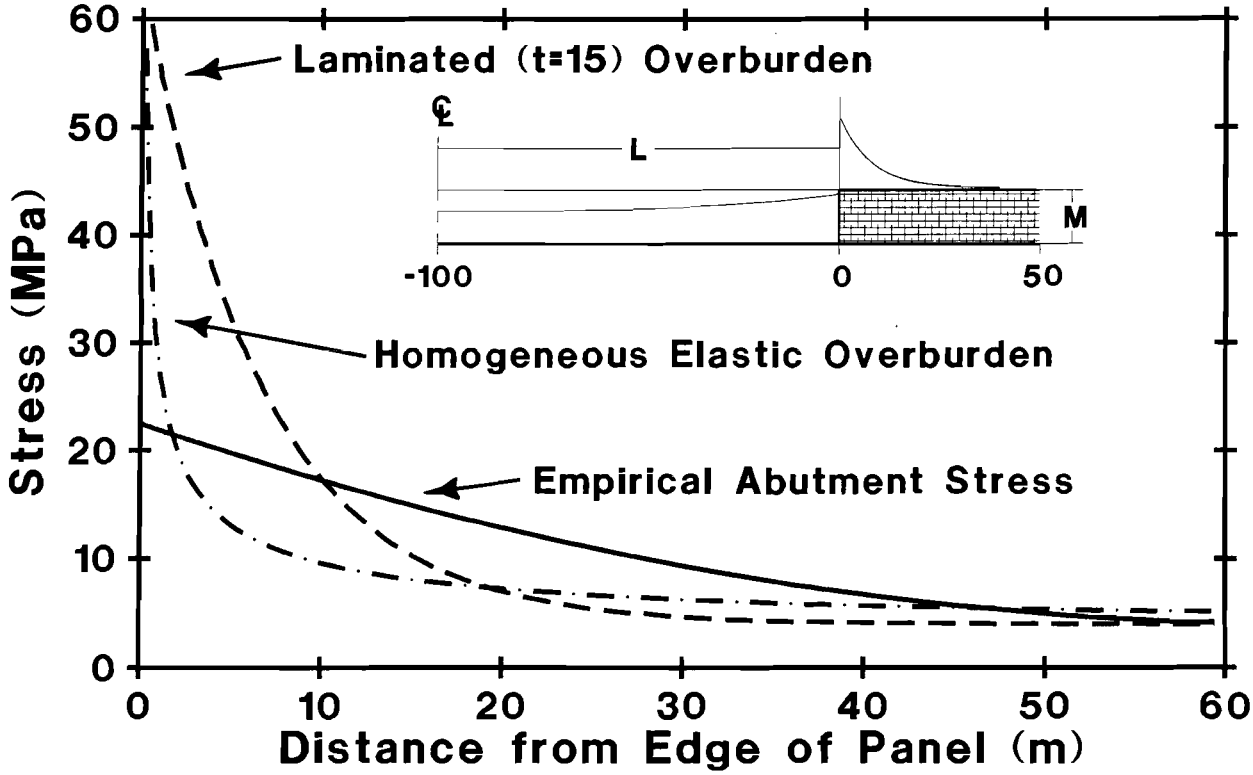

Figure 2.—Comparison of longwall abutment stress computed from the laminated and homogeneous isotropic models and from the empirical formula.

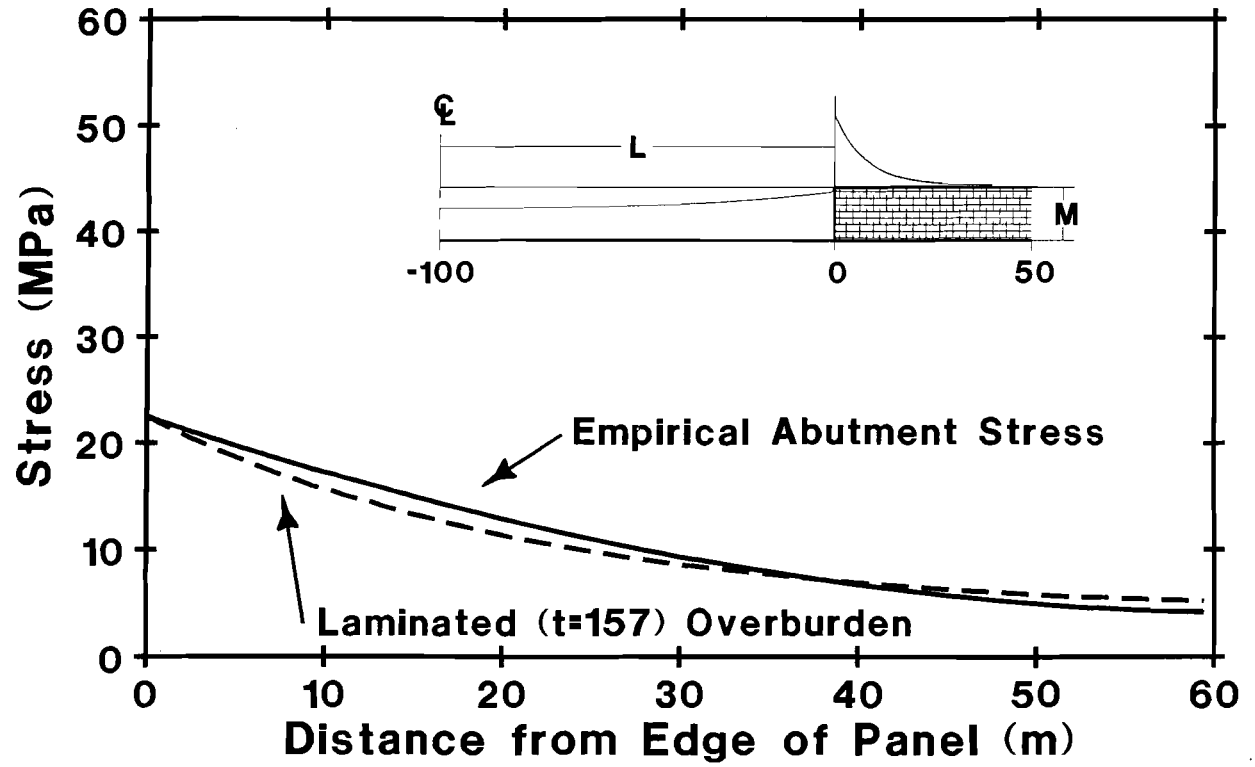

Figure 3.—Plot of the laminated abutment stress fitted to the empirical formula.

highlight the numerical flexibility provided by a variable lamination thickness parameter in the laminated model. (If a compressible seam is used, it may be possible to fit the abutment stress distribution in the homogeneous isotropic overburden to the empirical curve by varying the seam and overburden moduli. However, that calculation is beyond the scope of this paper.)

REMOTE DISPLACEMENTS

The next step was to analyze the remote displacements in the overburden generated by seam convergence. For the laminated overburden model, the kernel, or influence function, which relates the seam convergence (S_ℓ) to the vertical displacement (W_ℓ) of the overburden, was derived by Salamon [1962, 1989b] and Yang [1992]:

$$W_\ell(X,Y) = \frac{S_\ell}{4\sqrt{\pi\lambda Y}}\, e^{\frac{X^2}{4\lambda|Y|}}. \qquad (16)$$

Here, the magnitude of the convergence, S_ℓ, is assumed to occur over a unit element of the seam; the values of X and Y are the horizontal and vertical distances between the centroid of the converged seam element and the point in the overburden at which the displacement is desired.

Similarly, the kernel for the homogeneous isotropic overburden, which relates the seam convergence (S_h) to the vertical displacement (W_h) of the overburden, was derived by Crouch [1976] (see equation 17). Again, the magnitude of the convergence, S_h, is assumed to occur over a unit element of the seam, and the coordinates X and Y were defined previously in conjunction with equation 16. Note that the expression in equation 17 is again independent of elastic moduli.

Plots of the overburden displacements generated by these models are depicted in figure 4 for Y = 20 m (66 ft) and Y = 50 m (164 ft). In computing this illustration, a unit convergence spread over a seam element of unit length was assumed. Thus, the volume of convergence is identical in the two models. However, consistent with the greater suppleness of the laminated model, the stratified overburden (with a 15-m (49-ft) lamination thickness) appears to concentrate the displacement more tightly over the panel. This feature is particularly noticeable as the distance from the seam is increased.

This difference in remote displacement behavior is even more obvious in figure 5, which shows the 1-cm (0.39-in) displacement contours for both models generated above a unit volume convergence in a seam element. In this figure, the 1-cm (0.39-in) contour, or displacement "bulb," for the laminated model (with a 15-m (49-ft) lamination thickness) is broader and extends almost twice the distance into the overburden as the contour from the homogeneous elastic model. However, if the lamination thickness in the laminated model is increased to 28 m (92 ft)(as shown in figure 5), then the vertical extent of the 1-cm (0.39-in) displacement contour is equal between the two models, although the laminated displacement bulb is still broader. For most practical purposes (lower lamination thicknesses), both figures 4 and 5 indicate that seam displacements and stresses for a laminated overburden would propagate further and in a tighter pattern than the displacements and stresses from the homogeneous overburden. This greater remote response, coupled with the tendency for the laminated model to produce greater seam convergence, should greatly increase the remote displacements and stresses associated with a laminated displacement-discontinuity model.

SURFACE SUBSIDENCE

The final step in investigating the fundamental behavior of the laminated model was to analyze the surface subsidence over a longwall panel. In this analysis, the surface subsidence curves for the laminated and homogeneous isotropic models were calculated by taking the panel convergence from equations 6 and 7 and numerically integrating the surface subsidence using equations 16 and 17. These calculated subsidence curves are then compared in figure 6 with the results of the U.S. Bureau of Mines subsidence model [Jeran et al. 1986], which essentially represents an empirically derived "average" of 11 different subsidence curves from the Northern Appalachian Coal Basin.

For the subsidence curve of the laminated model in figure 6, the lamination thickness was optimized to provide the best fit with the empirical curve. This resulted in a lamination thickness of 5.3 m (17 ft), and from the figure, it can be seen that the laminated model provides a good fit to the empirical

$$W_h(X,Y) = \frac{S_h}{2\pi}\left(\arctan\left(\frac{Y}{X-0.5}\right) - \arctan\left(\frac{Y}{X+0.5}\right)\right) + \frac{S_h}{2\pi}\left(\frac{Y}{2(1-\nu)}\left(\frac{X+0.5}{(X+0.5)^2+Y^2} - \frac{X-0.5}{(X-0.5)^2+Y^2}\right)\right), \qquad (17)$$

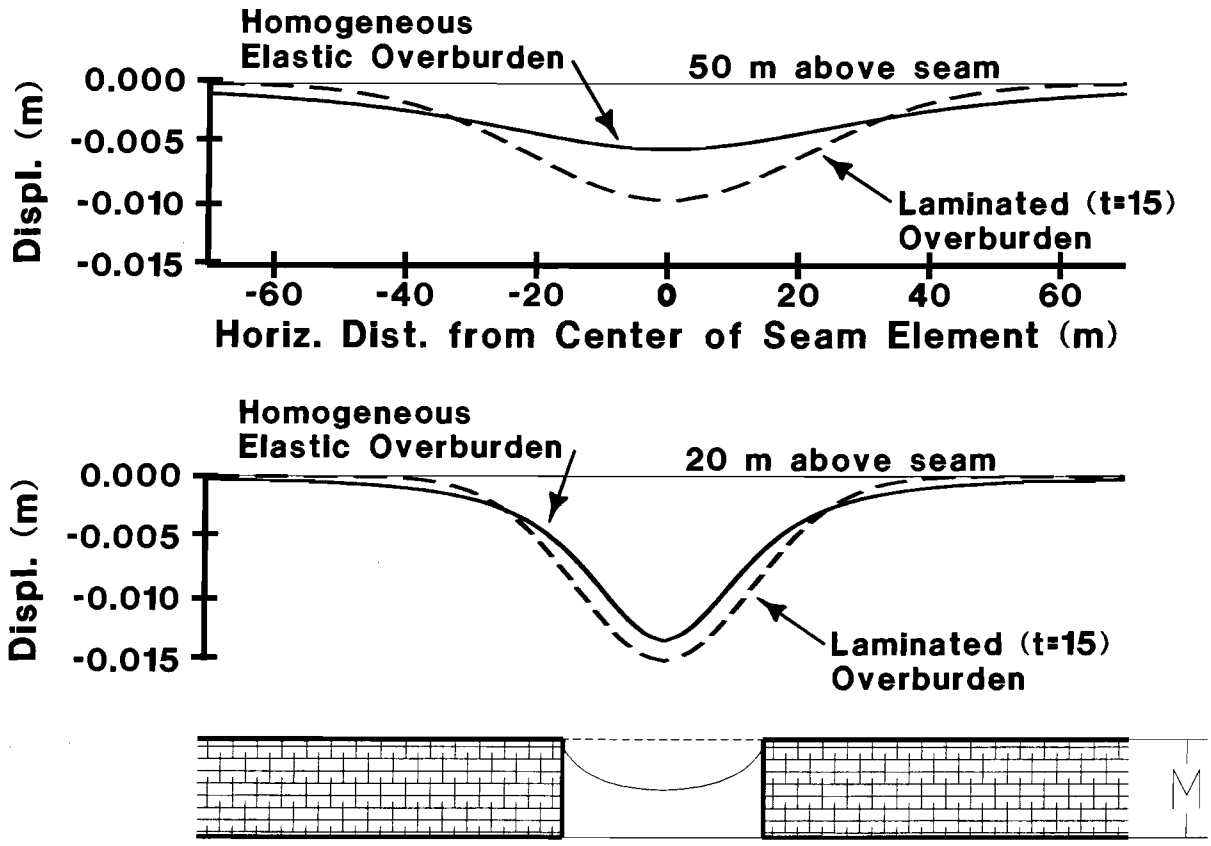

Figure 4.—Remote displacement due to a unit volume displacement.

curve. In earlier work where the laminated model was fit to several different individual sets of subsidence data [Yang 1992], a factor, ω:

$$\omega = \sqrt{\frac{H}{2\lambda}}, \qquad (18)$$

was found to be fairly constant at an average of 6.9. (Here, H is the overburden depth, and λ is defined in equation 5.) For the fitted subsidence curve from the laminated model in figure 6, the value of ω is 7.1, which agrees very well with this previous work.

For the subsidence curve from the homogeneous elastic overburden, the elastic modulus was lowered in an attempt to fit the empirical curve. However, long before the maximum surface subsidence from the model matched the maximum empirical surface subsidence, the convergence in the seam exceeded the seam thickness. The homogeneous elastic surface subsidence actually plotted in figure 6 was determined using an elastic modulus of 1 GPa (145,000 psi). From this curve, it is clear that the homogeneous isotropic surface subsidence is naturally much shallower and broader than the empirical data, and with only one effective variable parameter (E), the homogeneous isotropic model cannot be accurately fitted to the Northern Appalachian data. This result further confirms earlier indications that the homogeneous isotropic elastic overburden could not be made to fit subsidence data in the United Kingdom [Berry and Sales 1961; Salamon 1963].

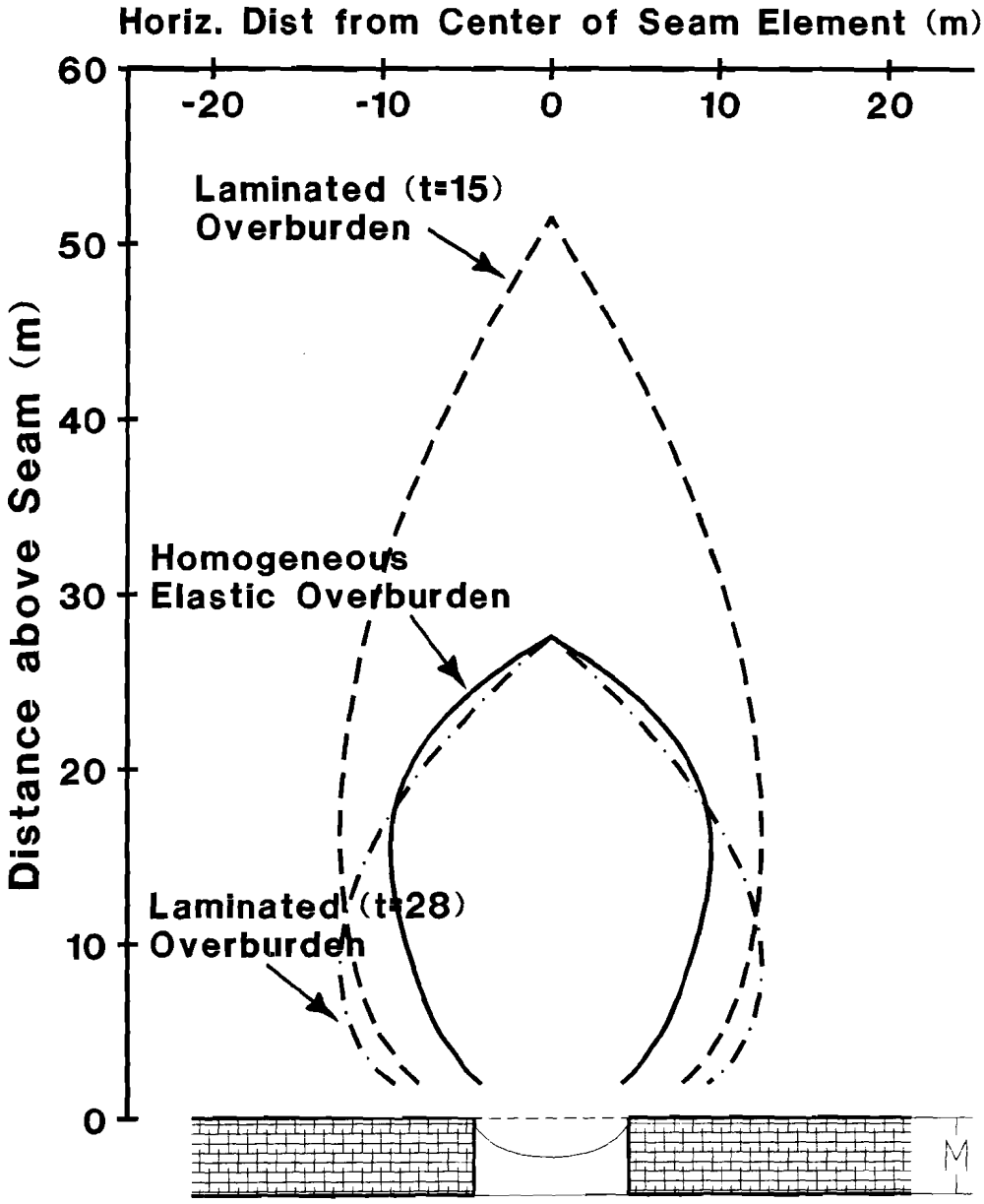

Figure 5.—1-cm (0.39-in) displacement contours associated with a unit volume displacement.

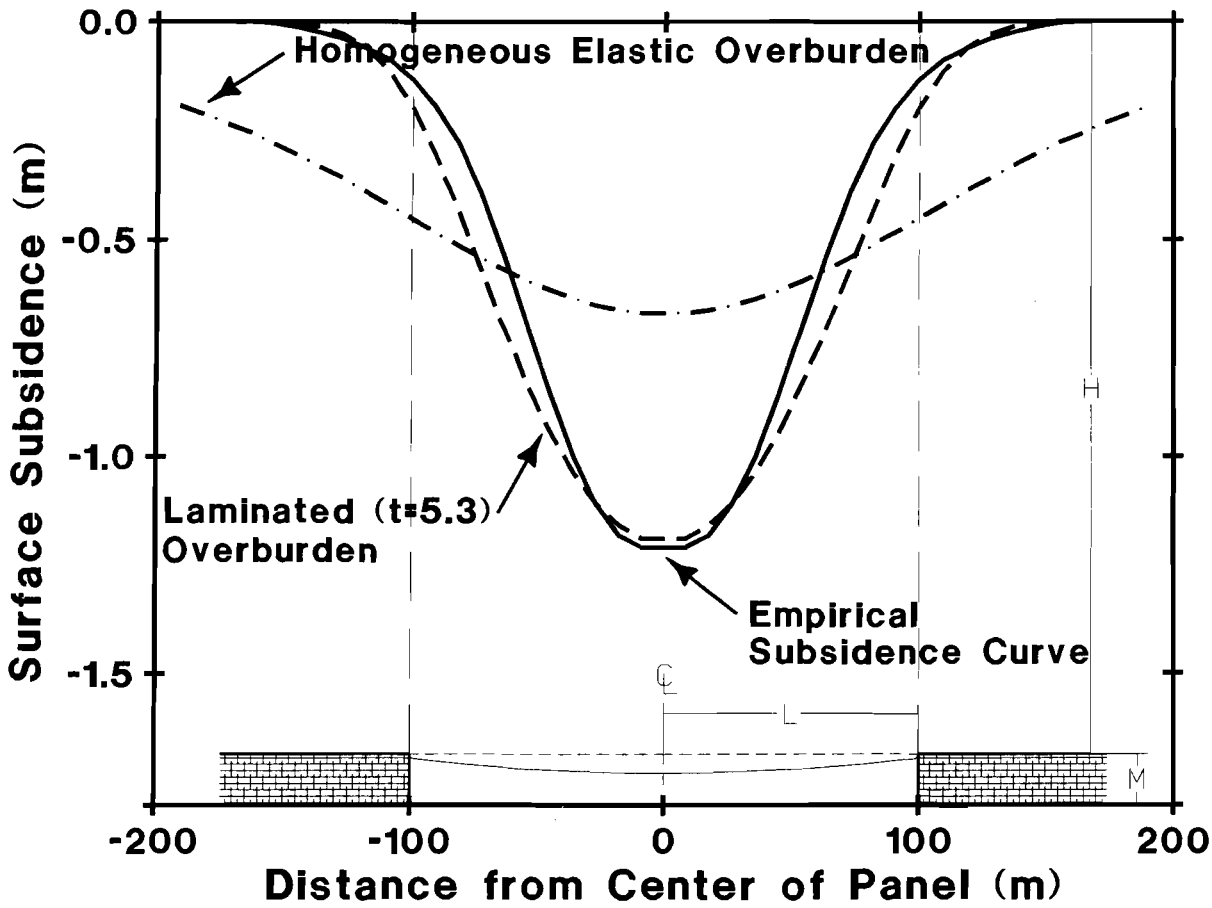

Figure 6.—Plot of the laminated and homogeneous isotropic subsidence fitted to the empirical curve.

THE LAMINATED MODEL PROGRAM, LAMODEL

IMPLEMENTATION FEATURES

The laminated overburden model, as presented in the previous sections of this paper, has been implemented into a modern boundary-element computer program called LAMODEL. This implementation has numerous practical features, including—

- Single- and multiple-seam simulations.
- Numerous individual excavation steps.
- Infinite media or surface effects for shallow seams.
- A constant overburden or a variable topography.
- Seam-level convergence and stress calculation, with each of the individual stress components (overburden, material, interseam, and surface) separately tabulated.
- User-defined laminae properties (elastic modulus, Poisson's ratio, and thickness).
- Up to 26 different in-seam materials can be specified from a selection of material models, which include elastic, elastic-plastic, strain-softening, bilinear strain-hardening, and exponential strain-hardening.
- User-defined convergence criteria.
- Grid sizes limited solely by the computation requirements (practical limit: 300 by 300).
- Either rigid or symmetric boundary conditions.
- Graphical pre- and postprocessors for simplified input entry and output analysis.

CASE STUDY

As part of the initial investigation and validation of this new implementation, the underground stresses, displacements, topographic stresses, and interseam interactions were modeled at a field site. This case study site is a multiple-seam situation

in eastern Kentucky. The geology in this area is fairly typical of the Southern Appalachian Coal Basin, with various sedimentary layers of sandstones, siltstones, shales, and numerous coal seams. The topography in the area is very rugged, with various steep ridges and valleys that have a topographic relief of over 600 m (2,000 ft). At the case study site, the overburden averages about 240 m (800 ft), but ranges from 90 m (300 ft) at the southeastern corner of the site to over 360 m (1,200 ft) at the northwestern corner (figure 7). (Because of the steep topography, it was critical to include the

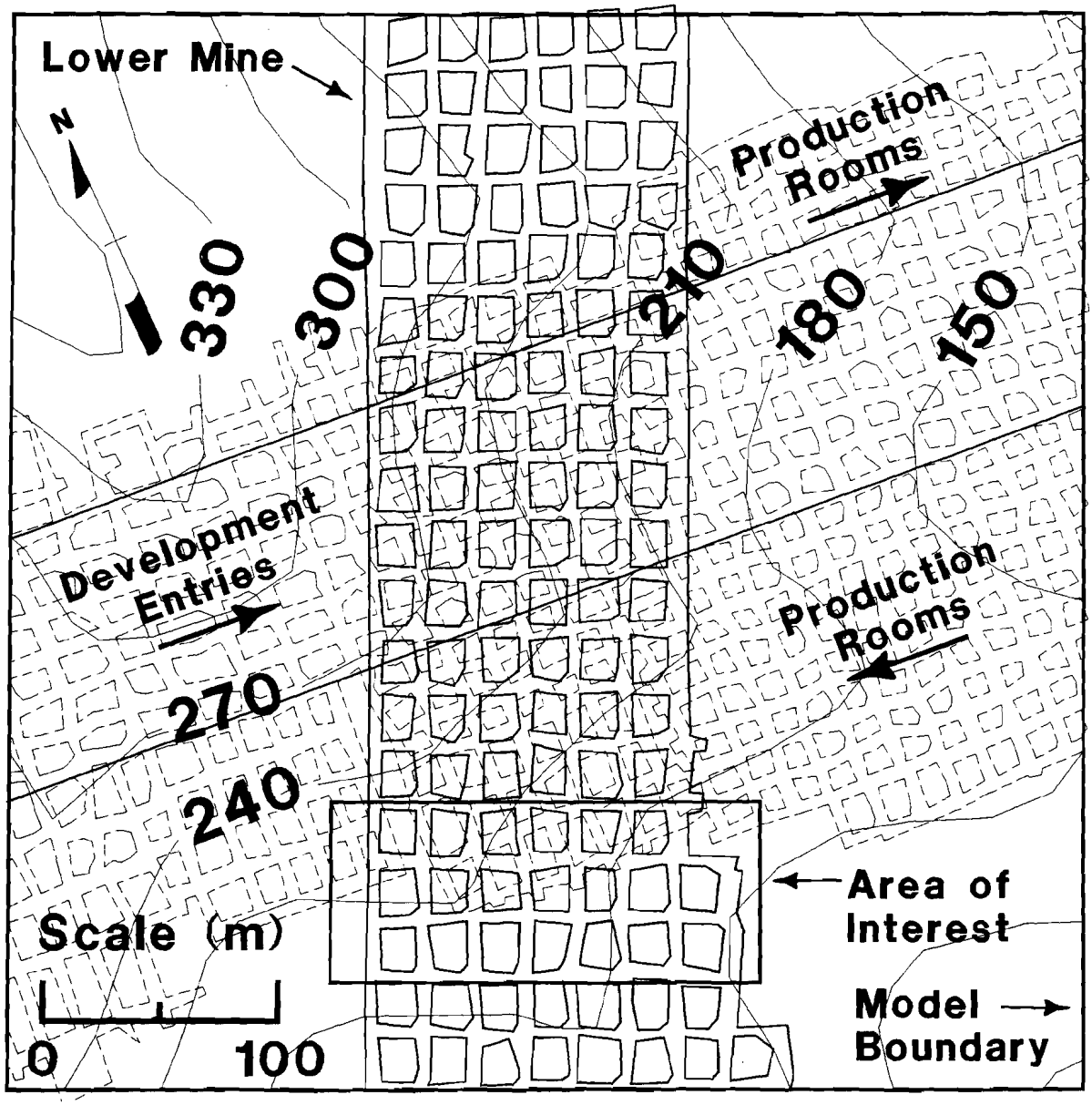

Figure 7.—Map of case study mines in eastern Kentucky.

topographic stress effects in the model to obtain accurate results.)

The overlying mine operates in the Upper Darby Seam, which typically averages about 2.0 m (6.5 ft) thick; however, in the model area, the extraction thickness had increased to over 2.7 m (9 ft). The lower mine operates in the Kellioka Seam, which averaged about 1.5 m (5.0 ft) thick in the study area. The interburden between the mines averages around 14 m (45 ft) and consists of interbedded sandstones and shales. The core logs nearest to the study site indicate about 3.5 to 5 m (12 to 15 ft) of thinly laminated shaley/carbonaceous sandstone (stack rock) directly over the Kellioka Seam. This is then overlain by 7.5 to 10.5 m (25 to 35 ft) of interbedded sandstones and shales, with shale primarily forming the floor of the Upper Darby Seam.

Both mines are room-and-pillar drift mines and utilize continuous miners for coal extraction. In some production sections, depending on local mining conditions, the mines remove the pillars on retreat for full extraction. In the study area, the lower mine had driven a seven-entry-wide set of main entries from north to south with pillars on 21- by 24-m (70- by 80-ft) centers and 6-m (20-ft) wide entries. Subsequently, the upper mine drove a seven-entry-wide set of panel development entries roughly perpendicular across the lower mains (figure 7). Relatively short (one- to two-crosscut) production rooms were driven to the north of the upper mine development entries during advance. At this point, no appreciable stress interaction was observed. Then, as the upper mine was pulling out of the section, long (seven- to eight-crosscut) production rooms with pillars on 18- by 18-m (60- by 60-ft), and smaller, centers were driven on the south side of the development entries (figure 7). At the extent of mining shown in figure 7, the upper mine began to experience major problems with pillar failure and floor heave and was forced to abandon the section.

Coincident with the failures in the upper mine, the lower mine experienced ground control problems in areas directly underlying the boundaries of the upper panel. These problems were primarily manifested as increased pillar spalling for approximately 30 m (100 ft) of entry and major roof cracking at overmined intersections. Both of these ground control problems were mitigated by supplemental bolting and cribbing.

The new laminated model, LAMODEL, was applied at this site to both quantify the magnitude of the stress interaction between the seams and to correlate the model results with in-mine ground control problems for subsequent predictions of mining conditions in future mine planning analysis. In the model, the seams were discretized with 3-m (10-ft) elements on 150-by-150 grids with the extent as shown in figure 7. Symmetrical seam boundary conditions were set, and no free-surface effects were included. The interburden was set at 14 m (45 ft), and the rock mass was simulated with a modulus of 20,700 MPa (3 million psi) and 15-m (50-ft) thick laminations. A strain-softening material was used for the in-seam coal, and the peak strength of the coal was varied until the pillars in the upper seam had just reached failure.

Additionally, because of the high topographic relief at the site, the topography was discretized with 15-m (50-ft) elements for an area extending 300 m (1,000 ft) beyond the limits of the displacement-discontinuity grids. The importance of including the topographic stress effects in the model is clearly evident in figure 8, which shows the topographic stress at the level of the upper mine. It is interesting to note in this figure the amount to which the topographic stress is "smoothed" with depth in comparison with the original topography shown in figure 7. Also, it should be observed in figure 8 that near the boundary of the upper mine (the area of interest) the topographic stress varies about 1.4 MPa (200 psi), or 30%, across the pillars in the lower mine.

The primary results of this multiple-seam modeling effort are shown in figure 9. Figure 9*C* shows the stress concentrations on the lower seam resulting from the pillar failure in the upper seam. In this image, stress concentrations up to 4.5 MPa (650 psi) and with functional widths of between 9 to 37 m (30 to 120 ft) can be seen. This model response correlates well with the underground observations. The calculated seam interaction stress results in increases of the average pillar stress in the lower mine up to 55% (figures 9*A* and 9*B*). By correlating this 55% increase in pillar stress with the observed ground control problems underground (figure 9), the magnitude of future ground control problems at this site can now be more accurately determined using LAMODEL.

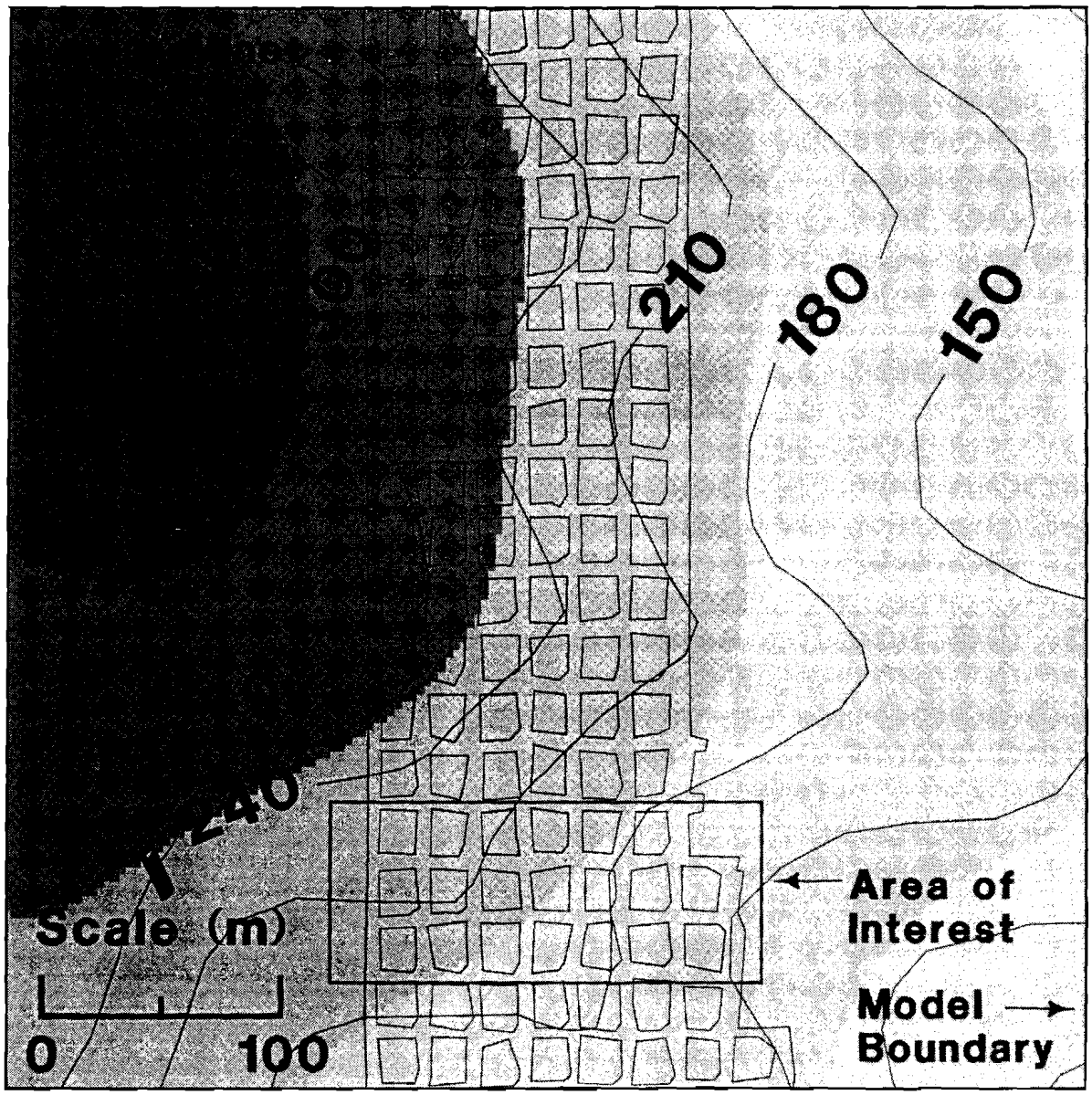

Legend (MPa)

2.0	3.4	4.8	6.2	7.6	9.0

Figure 8.—Topographic stress on lower seam.

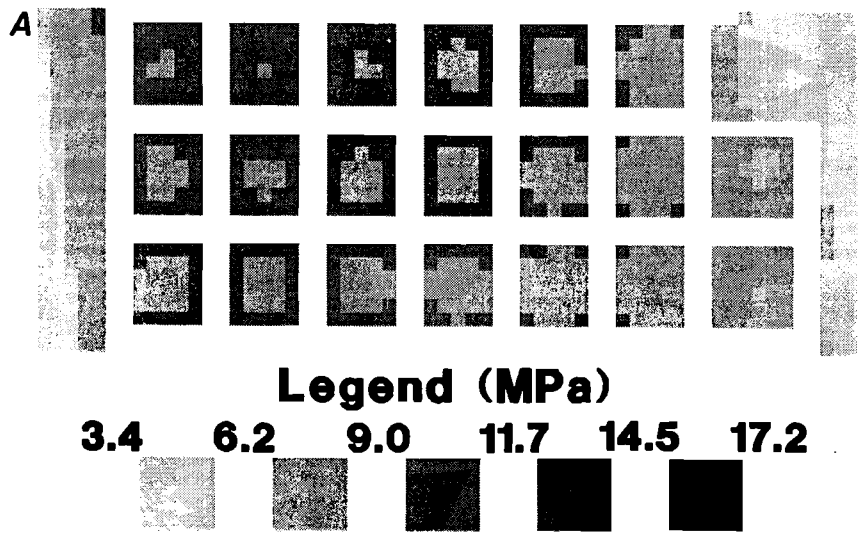

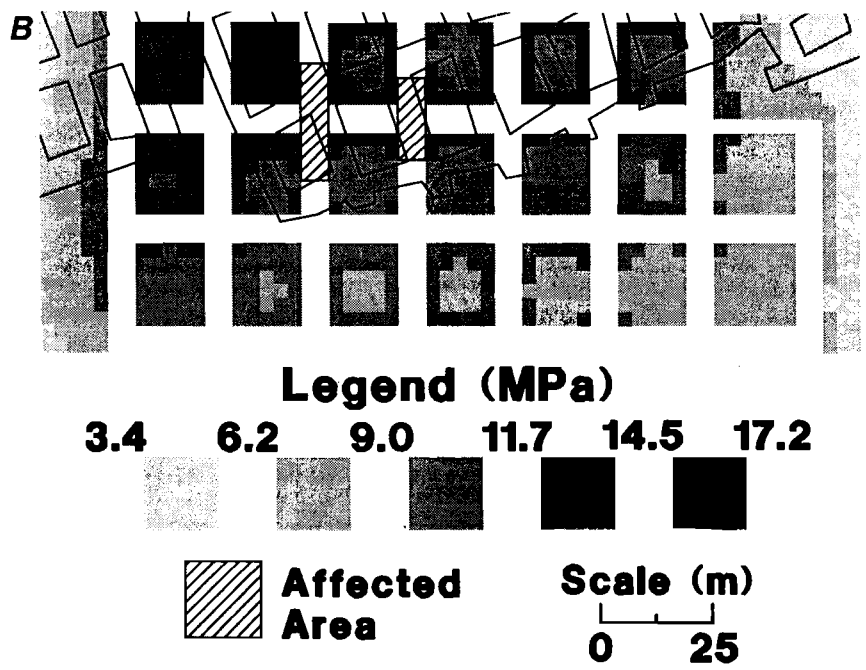

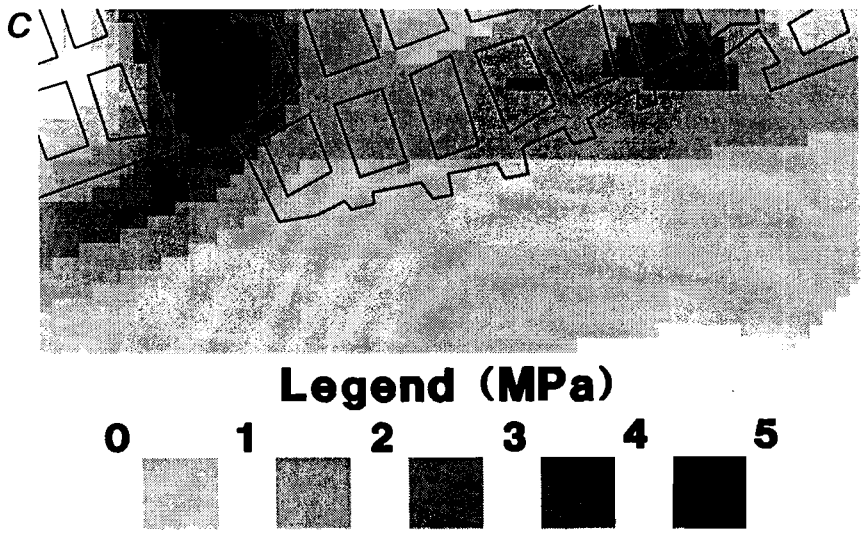

Figure 9.—Stress analysis on lower mine. *A*, single-seam stress; *B*, multiple-seam stress; *C*, additional stress from upper seam.

SUMMARY AND CONCLUSIONS

The investigation of the fundamental behavior of the laminated overburden presented in the first part of this paper has produced a number of significant results. First, it is clear that the laminated overburden (with a low lamination thickness) is more flexible or supple than the homogeneous isotropic overburden. This increased suppleness is evident in the greater convergence across a longwall panel, in the larger extent of the remote displacement contours, and in the nature of the surface subsidence. Second, due to the larger extent of the remote displacement contours, it is clear that a multiple-seam mine model using the laminated overburden will show increased interseam displacements and stresses compared with a homogeneous isotropic overburden. Third, because the overburden in the laminated model is effectively described with two parameters (as opposed to one parameter in the homogeneous isotropic model) and therefore provides two degrees of freedom for fitting observed data, the laminated model was capable of closely matching the observed abutment stresses and surface subsidence. In fact, the laminated model was easily fit to the observed surface subsidence, whereas the subsidence for the homogeneous isotropic overburden was fundamentally different from the observed subsidence.

In the second part of this paper, a new laminated displacement-discontinuity program, LAMODEL, was presented. This new program, in addition to the laminated overburden, also implements a number of innovative features, including topographic stress calculations, various in-seam material models, and variable boundary conditions at the seam level. In order to evaluate the accuracy and utility of the new model, it was used in a case study of a multiple-seam mining situation in steep topography. At this site, the ability of LAMODEL to include topographic stress effects, strain-softening coal, and symmetric boundary conditions greatly increased the realism and accuracy of the model. By correlating the LAMODEL results with the observed ground control problems, mine management will be better able to design and plan for future multiple-seam interactions. Because of the realistic flexibility of the laminated overburden model and the utility of the numerous practical features implemented in the new program, it appears that LAMODEL can provide realistic stress and displacement calculations for a wide range of mining situations.

REFERENCES

Berry DS [1960]. An elastic treatment of ground movement due to mining - part I. Isotropic ground. J Mech Physics of Solids *8*:280-292.

Berry DS, Sales TW [1961]. An elastic treatment of ground movement due to mining - part II. Transversely isotropic ground. J Mech Physics of Solids *9*:52-62.

Cook NGW, Hoek E, Pretorious JPG, Ortlepp WD, Salamon MDG [1966]. Rock mechanics applied to the study of rock bursts. J South Afr Inst Min Metall *66*:436-528.

Crouch SL [1976]. Analysis of stresses and displacements around underground excavations: an application of the displacement discontinuity method. Minneapolis, MN: University of Minnesota, Department of Civil Engineering, Geomechanics Report.

Crouch SL, Fairhurst C [1973]. The mechanics of coal mine bumps and the interaction between coal pillars, mine roof, and floor. U.S. Department of the Interior, Bureau of Mines, OFR 53-73.

Heasley KA, Zelanko JC [1992]. Pillar design in bump-prone ground using numerical models with energy calculations. In: Iannacchione AT, Mark C, Repsher RC, Tuchman RJ, Jones CC, comp. Proceedings of the Workshop on Coal Pillar Mechanics and Design. Pittsburgh, PA: U.S. Department of the Interior, Bureau of Mines, IC 9315, pp. 50-60.

Jaeger JC, Cook NGW [1979]. Fundamentals of rock mechanics. London: Chapman and Hall.

Jeran PW, Adamek V, Trevits MA [1986]. A subsidence prediction model for longwall mine design. In: Proceedings of the Longwall U.S.A. Conference. Pittsburgh, PA: pp. 101-112.

Kripakov NP, Beckett LA, Donato DA, Durr JS [1988]. Computer-assisted mine design procedures for longwall mining. Pittsburgh, PA: U.S. Department of the Interior, Bureau of Mines, RI 9172.

Mark C [1990]. Pillar design methods for longwall mining. Pittsburgh, PA: U.S. Department of the Interior, Bureau of Mines, IC 9247.

Plewman RP, Deist FH, Ortlepp WD [1969]. The development and application of a digital computer method for the solution of strata control problems. J South Afr Inst Min Metall *70*(9):33-44.

Salamon MDG [1961]. An introductory mathematical analysis of the movements and stresses induced by mining in stratified rocks. Durham, United Kingdom: King's College, University of Durham, Department of Mining, Research Report *9*:Bull 3.

Salamon MDG [1962]. The influence of strata movement and control on mining development and design [Thesis]. Durham, United Kingdom: University of Durham, Department of Mining.

Salamon MDG [1963]. Elastic analysis of displacements and stresses induced by the mining of seam or reef deposits, part I. J South Afr Inst Min Metall *63*(4):128-149.

Salamon MDG [1964]. Elastic analysis of displacements and stresses induced by the mining of seam or reef deposits, part II. J South Afr Inst Min Metall *64*(6):197-218.

Salamon MDG [1974]. Rock mechanics of underground excavations. In: Proceedings of the 3rd Congress, International Society for Rock Mechanics. Denver, CO: National Academy of Sciences, *1*(b)951-1099.

Salamon MDG [1989a]. Some applications of the frictionless laminated model. In: Proceedings of the 30th U.S. Symposium on Rock Mechanics. Morgantown, WV: West Virginia University, pp. 891-898.

Salamon MDG [1989b]. Subsidence prediction using a laminated linear model. In: Proceedings of the 30th U.S. Symposium on Rock Mechanics. Morgantown, WV: West Virginia University, pp. 503-510.

Salamon MDG [1991]. Deformation of stratified rock masses: a laminated model. J South Afr Inst Min Metall *91*(1):9-26.

Sinha KP [1979]. Displacement discontinuity technique for analyzing stresses and displacements due to mining in seam deposits [Thesis]. Minneapolis, MN: University of Minnesota.

Yang G [1992]. Numerical approach to the prediction of subsidence due to longwall coal mining using a laminated model [Thesis]. Golden, CO: Colorado School of Mines.

Zipf RK Jr., Heasley KA [1990]. Decreasing coal bump risk through optimal cut sequencing with a non-linear boundary element program. In: Hustrulid WA, Johnson GA, eds. Proceedings of the 31st U.S. Symposium on Rock Mechanics. Golden, CO: Colorado School of Mines, pp. 947-954.

NIOSH

IC 9446 INFORMATION CIRCULAR/1997

Proceedings: New Technology for Ground Control in Retreat Mining

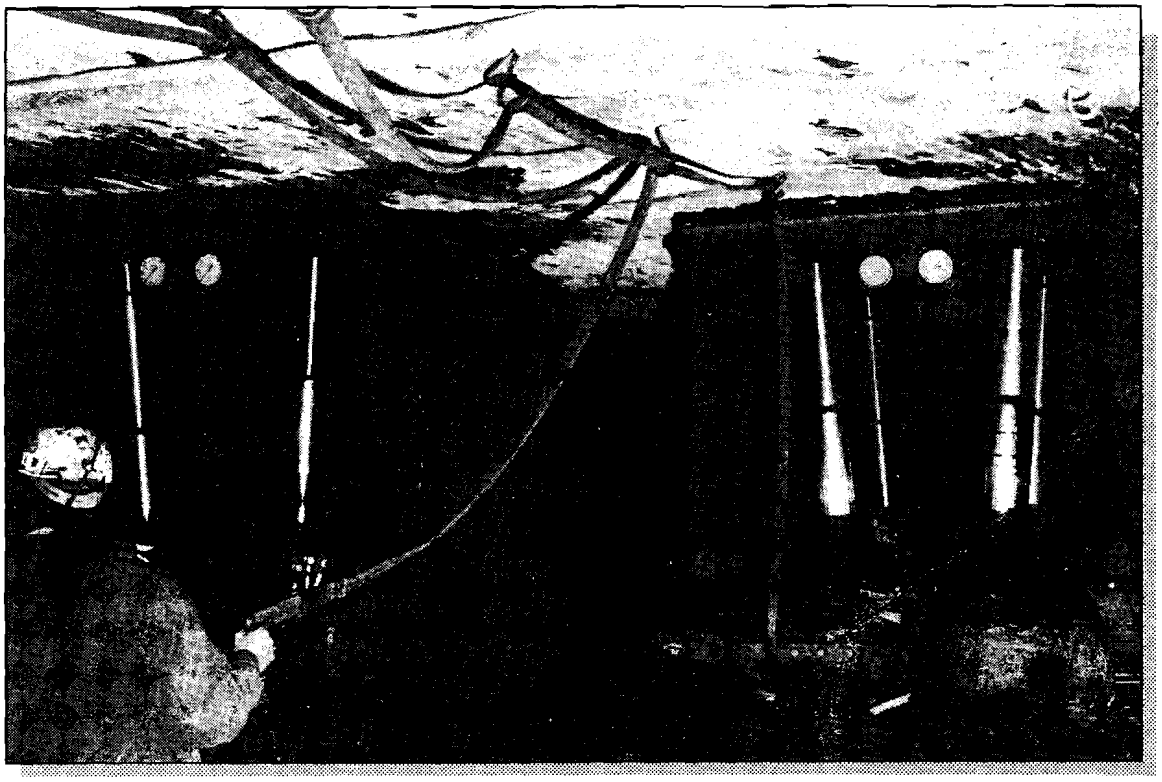

U.S. DEPARTMENT OF HEALTH AND HUMAN SERVICES
Public Health Service
Centers for Disease Control and Prevention
National Institute for Occupational Safety and Health

CDC
CENTERS FOR DISEASE CONTROL AND PREVENTION

Cover photo: Pillar extraction using mobile roof supports.

Information Circular 9446

Proceedings: New Technology for Ground Control in Retreat Mining

Christopher Mark, Ph.D., and Robert J. Tuchman

U.S. DEPARTMENT OF HEALTH AND HUMAN SERVICES
Public Health Service
Centers for Disease Control and Prevention
National Institute for Occupational Safety and Health
Pittsburgh, PA and Spokane, WA Research Centers

March 1997

International Standard Serial Number
ISSN 1066-5552

CONTENTS

PILLAR DESIGN

MOBILE ROOF SUPPORTS

UNIT OF MEASURE ABBREVIATIONS USED IN THIS REPORT

cm	centimeter	lbf	pound (force)
ft	foot	m	meter
ft/min	foot per minute	m/min	meter per minute
ft^2	square foot	m^2	square meter
ft^3	cubic foot	m^3	cubic meter
GPa	gigapascal	min	minute
ha	hectare	mm	millimeter
in	inch	MPa	megapascal
in^2	square inch	psi	pound (force) per square inch
kg	kilogram	st	short ton
kips/in	kips per inch	st/h	short ton per hour
kN	kilonewton	t	ton (metric)
kN/cm	kilonewton per centimeter	%	percent
kPa	kilopascal	°	degree
lb	pound		

Mention of any company name or product does not constitute endorsement by the National Institute for Occupational Safety and Health.

To receive other information about occupational safety and health problems, call
1-800-35-NIOSH (1-800-356-4674), or
visit the NIOSH Home Page on the World Wide Web at
http://www.cdc.gov/niosh/homepage.html

DISCLAIMER OF LIABILITY

The National Institute for Occupational Safety and Health expressly declares that there are no warranties, express or implied, that apply to the software described herein. By acceptance and use of said software, which is conveyed to the user without consideration by the National Institute for Occupational Safety and Health, the user hereof expressly waives any and all claims for damage and/or suits for or by reason of personal injury or property damage, including special, consequential, or other similar damages arising out of or in any way connected with the use of the software described herein.